Supporting Information

Djurec et al. 10.1073/pnas.1717802115

SI Materials and Methods

Tumor Monitoring and Perfusion Assay by Micro-Ultrasound. Mice were anesthetized with 4% isoflurane (Braun Vet Care) in 100% oxygen at a rate of 1.5 L/min. Hypothermia associated with anesthesia was avoided using a bed-heater. Abdominal hair was removed by depilation cream to prepare the examination area. Mice were screened for PDAC, and tumors were measured with the Vevo 770 micro-ultrasound system (VisualSonics) with an ultrasound transducer of 40 MHz (RMV704; VisualSonics). PDAC size was calculated as length × width^2/2. The tumor perfusion and vascularization study was performed by administration of MicroMarker Contrast agent (VisualSonics).

Treatments. Mice were treated i.p. twice weekly with gemcitabine (Gemzar, Eli-Lilly) (100 mg/kg) or saline, 100-μL volume. Combination treatments of gemcitabine and anti-VEGF monoclonal antibody B20 4.1.1 (5 mg/kg) (Genentech) or the macrophage-depleting agent clodronate (50 mg/kg clodronate liposomes) were administered i.p. at the same time. Tumor growth was followed weekly by microultrasound. Mice were treated until the humane end point to study survival.

Histopathology, Immunohistochemistry, and Digital Image Analysis. For histological analyses, tissues were fixed in 10% buffered formalin and embedded in paraffin. H&E staining and immunohistochemical (IHC) analyses were performed on 3-μm paraffin sections. For IHC, the following antibodies were used: anti-mouse CD31 (1:50; Abcam); anti-mouse F4/80 (1:20; CI: A3-1; ABD Serotec); anti-mouse CK19 (TROMA III; CNIO Monoclonal Antibody Unit); anti-mouse Ki67 (SP6; Master Diagnostica); GFP mouse monoclonal (1:500; Roche); anti-mouse cleaved caspase 3 (Asp-175l) (1:750; 9661; Cell Signaling), anti-mouse phospho-histone H3 (Ser10) (1:500; Millipore), anti-mouse CD3 (1:250) (M20; Santa Cruz Biotechnology), anti-mouse MPO (1:1,250; A0398; Dako), and anti-mouse Pax5 (1:500; C-20; Santa Cruz Biotechnology). Digital images of immunostained slides were obtained at 40× magnification (0.12 μm per pixel) using a whole-slide scanner (MIRAX scan; Zeiss) fitted with a 40×/0.95 Plan Apochromat objective lens (Zeiss). Images were analyzed by ZEN2 software. At least four tumors were sectioned, and one section was analyzed for quantification of each staining.

Immunofluorescence and Confocal Imaging. CAFs and NPFs (5×10^5 cells per well) were plated in 24-well plates using BioCoat Poly-D-Lysin (Cellware) coverslips and were allowed to grow for 24 h. Tissue samples were sectioned (10 μm) by cryostat from optimum cutting temperature (OCT) compound blocks. Samples were fixed in 4% paraformaldehyde (Electron Microscopy Sciences). Permeabilization was performed by 0.2% Triton X-100 solution. Primary antibodies, including those elicited against αSMA (1:100; Biocare Medical) and anti-mouse PDGFRα (CD140a; 1:100; clone: APA5; eBioscience), were incubated overnight at 4 °C followed by the addition of the secondary antibody, Alexa Fluor 594 at 1:200 for 1 h at room temperature; then Hoechst (Invitrogen) staining was applied. Sections were mounted with Mowiol. Captures were performed with a TCS SP5 confocal microscope (Leica Microsystems) equipped with 20× NA, 0.7 dry, 20× 0.7 multi-immersion, and 40× NA 1.25 oil objectives. Leica AF software was used for acquiring and processing the images.

Flow Cytometry Analysis. Cells were trypsinized and immunostained with APC-Cy7 anti-mouse αSMA (1:75; Abcore) and phycoerythrin (PE) anti-mouse CD140a (PDGFRα; 1:100; clone: APA5; eBioscience). For the CSC population PE anti-mouse CXCR4 (1:100; clone: 2B11; BD Biosciences), APC anti-mouse CD133 (1:100; clone:13A4; eBioscience), PE-Cy7 anti-mouse CD44 (1:100; clone: IM7), and FITC anti-mouse CD326 (EpCAM; 1:200; clone: G8.8; BioLegend) were used. For monocyte/macrophage profiling, anti-mouse F4/80 (1:100; clone: BM8; eBioscience), anti-mouse PE-Cy7 CD11b (1:100; clone: M1-70; BD Biosciences), PerCP-Cy5.5 anti-mouse CD11c (1:100; clone: N418; eBioscience), and anti-mouse CD206 PE (1:50; Serotec) were used. Samples were processed on a FACS CANTO II flow cytometer (BD Pharmingen) and analyzed using FlowJo (Tree Star).

Mouse CAFs, NPFs, and Tumor-Cell Cultures. Fibroblasts isolated from mouse PDAC tumors or healthy pancreata were plated at high density and cultured in DMEM supplemented with 10% FBS. Tumor cells were isolated by cell sorting using EYFP expression as a marker and were plated and maintained in DMEM supplemented with 10% FBS. Fibroblast and tumor cell cultures were used at early passages.

Human CAFs and NPFs Culture. Fibroblasts from human PDAC tumors or adjacent normal pancreas were isolated by outgrowth as previously described (63). Briefly, tissue samples were cut into 2-mm^3 slices and were cultured in DMEM with 10% FBS until all other cell types failed to survive or propagate.

Organoid Cocultures and Quantification. Organoids were established from tumor tissues obtained from KPeCY mice at the humane end point based on a previously described protocol (64). Fibroblasts were plated (1×10^5) in 24-well glass-bottomed plates (Greiner Bio-One). Organoids were passed at 1:6 dilution from confluent 24-well plates. Organoids were cocultured with fibroblast in basic medium without factors (Advanced DMEM + Hepes + GlutaMAX) for 5 d. Images were acquired in a Leica DMI6000B wide-field microscope (Leica Microsystems) equipped with a 5× NA, 0.15 dry objective and an incubator chamber at 37 °C and 5% CO_2. Leica AF and Leica HCS-A software were used for the acquisition.

Migration and Wound-Healing Assays. Cells were allowed to grow in 10% FBS containing DMEM to confluence in six-well plates. Three vertical 1-mm-wide scratches were made across the cell layer using a sterile pipette tip. After washing in PBS, serum-free DMEM was added (65). Wound-healing assays were acquired in a Leica DMI6000B wide-field microscope (Leica Microsystems). Images were acquired with the bright-field method every 10 min for 20 h and were processed by Fiji software.

shRNA-Mediated Knockdown. For *Mpp6*-knockdown assays, cells were infected using lentiviral particles generated with Mission-shRNA plasmids TRCN0000361747 (Sigma). Nontarget shRNA control vector (sh-Ctrl) was used as a negative control.

qRT-PCR. Total RNA was extracted with the RNeasy Mini Kit (QIAGEN) and was reverse-transcribed using Super Script II Reverse Transcriptase (Invitrogen) and random primers (Invitrogen) following the manufacturer's instructions. The qRT-PCR assays were performed with a FAST7500 Real-Time PCR System using Power SYBR Green PCR Master Mix (Applied Biosystems) with the primers indicated below. GAPDH was used for normalization.

Primers for *Saa1* amplification:

5-AGGAGACACCAGGATGAAGC-3 (forward)

5-GGAAAGCCTCGTGAACAAAT-3 (reverse)

Primers for *Saa2* amplification:

5-CCACAAGCCTCTCTCTGTGA-3 (forward)

5-AGTTCCCTGTTTCCATCGAC-3 (reverse)

Primers for *Saa3* amplification:

5-TGCCATCATTCTTTGCATCT-3 (forward)

5-AGTAGGCTCGCCACATGTCT-3 (reverse)

Primers for *CD68* amplification:

5-AGCCATTCAAGACAAAGCCT-3 (forward)

5-CAAGGTGAACAGCTGGAGAA-3 (reverse)

Primers for *CK19* amplification:

5-TGTCGACCTAGCCAAGATCC-3 (forward)

5-AAGGTAGGTGGCTTCAGCAT-3 (reverse)

Primers for *Vimentin* amplification:

5-CGGCTGCGAGAGAAATTGC-3 (forward)

5-CCACTTTCCGTTCAAGGTCAAG-3 (reverse)

Primers for *FAP* amplification:

5-TTTCCAGGCGATGTGGTACT-3 (forward)

5-ATGGTCCAAGTCGTCCATGT-3 (reverse)

Primers for *PDGFRβ* amplification:

5-AGCCAGAAGTAGCGAGAAGC-3 (forward)

5-GGCAGTATTCCGTGATGATG-3 (reverse)

Primers for *Mpp6* amplification:

5-GATCTGGTAATCGCCCGAATC-3 (forward)

5-GGTGCCTCTCCATATTGACGTA-3 (reverse)

Primers for *GAPDH* amplification:

5-CGACTCAGATGTCCCTGGAT-3 (forward)

5-GCCTGTCCAAGCAATGAAAT-3 (reverse)

Statistical and Data Analysis. Data are expressed as mean ± SD except for FACS analysis, for which representative images were used. Significance between two groups was assessed by the Student's two-tailed *t* test. Datasets consisting of more than two groups were analyzed by analysis of variance (ANOVA). The Kaplan–Meier product limit method was used for generating the survival curves, which were compared by using the log-rank (Mantel–Cox) test. Differences in metastasis appearance between two groups were analyzed by χ^2 test. P values < 0.05 were considered statistically significant ($^{*}P < 0.05$; $^{**}P < 0.001$; $^{***}P < 0.001$). All statistical analysis was performed using GraphPad Prism software.

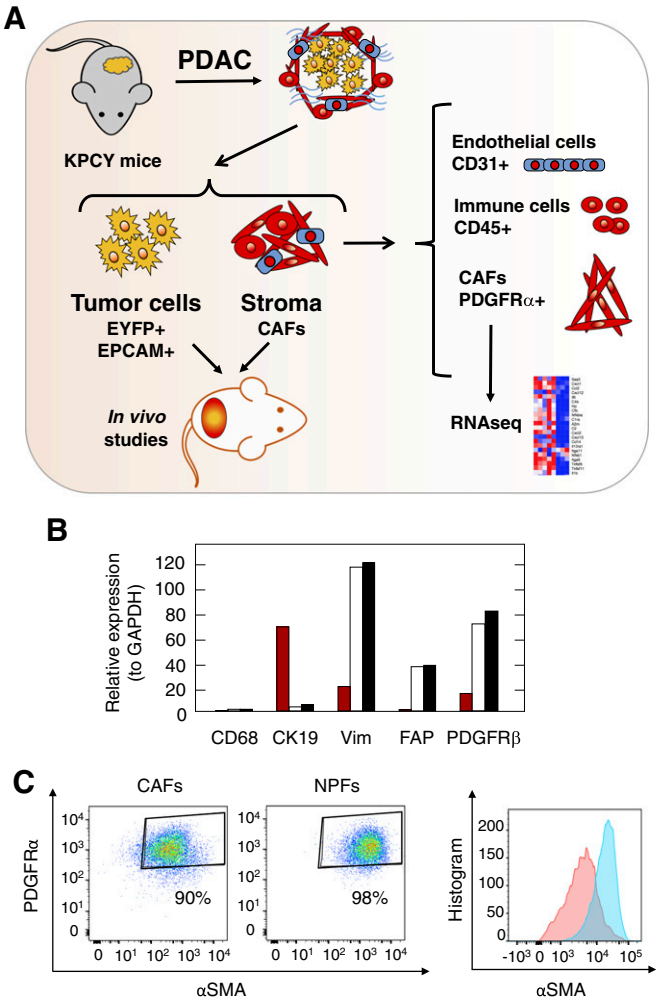

Fig. S1. (*A*) Schematic diagram of the strategy followed in this study to sort the different cell populations from GEM PDAC tumors. Immune cells were separated by CD45 expression, endothelial cells by CD31 staining, tumor cells by the EYFP marker and EpCAM-FITC staining, and CAFs by PDGFRα expression. Cells were used for cell culture, RNAseq, and in vivo tumor growth studies. (*B*) Expression levels of CD68 (immune cell marker), CK19 (tumor cell marker), and Vimentin (Vim), FAP, and PDGFRβ (fibroblast markers) analyzed by qPCR (relative to GAPDH expression) in tumor cells (red bars), NPFs (open bars), and CAFs (black bars). (*C*, *Left*) A representative FACS analysis of αSMA/PDGFRα coexpression in CAFs and NPFs. (*Right*) FACS histogram representing the αSMA expression intensity in CAFs (red) and NPFs (blue).

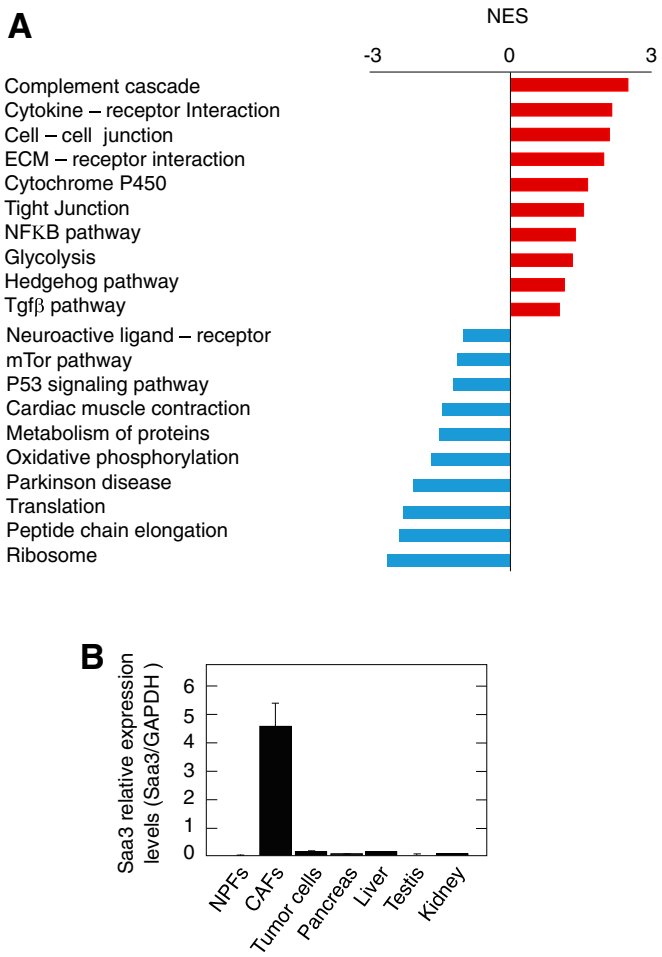

Fig. S2. (*A*) GSEA pathway analysis illustrating 10 significantly up- and down-regulated pathways in CAFs. The NES ranking was generated by the GSEA. (*B*) Saa3 expression levels analyzed by qPCR (relative to GAPDH expression) in NPFs, CAFs, tumor cells, and the indicated normal tissues.

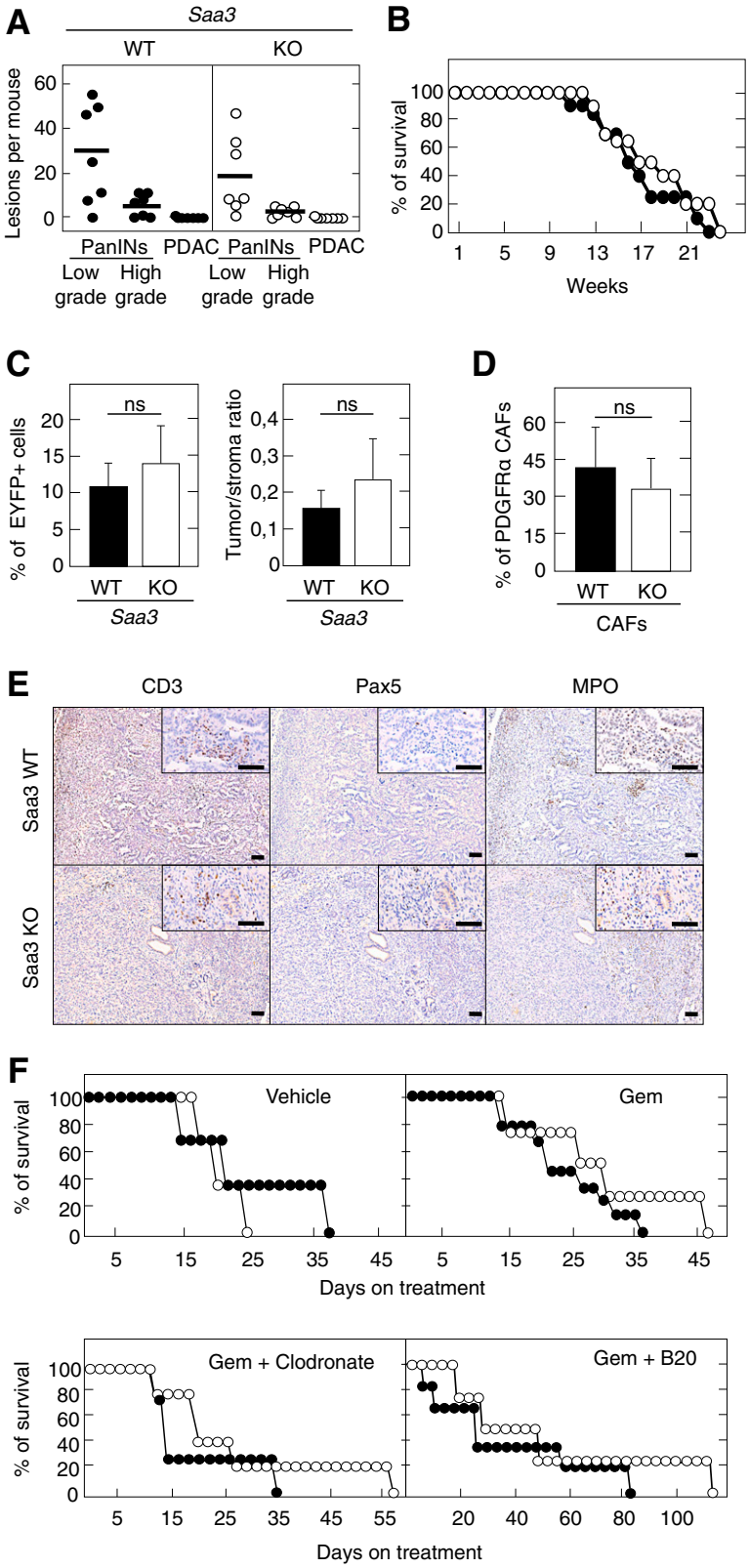

Fig. S3. (*A*) Quantification of low- and high-grade PanIN lesions and PDACs in 1-y-old *Saa3*-competent (solid circles) and *Saa3*-null (open circles) K-*Ras*$^{+/LSLG12Vgeo}$; *Elas*-tTA/*tetO*-Cre;*Rosa26*$^{+/EYFP}$ mice ($n = 7$ for both genotypes). (*B*) Kaplan–Meier survival analysis of *Saa3*-competent (solid circles) and *Saa3*-null (open circles) KPeCY mice. (*C*) Quantitative FACS analysis of EYFP$^+$ tumor cells (*Left*) and tumor/stroma ratio in PDAC tumors (*Right*) of *Saa3*-competent (solid bars) and *Saa3*-null (open bars) KPeCY mice ($n = 6$). The tumor/stroma ratio was calculated as the percentage of tumor cells vs. the percentage of immune (CD45$^+$), endothelial (CD31$^+$), and fibroblast (PDGFRα$^+$) compartments all together ($n = 6$). (*D*) Quantitative FACS analysis of PDGFRα$^+$ cells in PDAC tumors of *Saa3*-competent (solid bars) and *Saa3*-null (open bars) KPeCY mice. (*E*) Representative images of IHC staining of CD3 (T lymphocytes), Pax5 (B lymphocytes), and myeloperoxidase (MPO) (neutrophils) in *Saa3*-competent (WT) and *Saa3*-null (KO) tumors. (Scale bars, 50 μm.) (*F*) Kaplan–Meier survival analysis of *Saa3*-competent (solid circles) and *Saa3*-null (open circles) tumor-bearing KPeCY mice after exposure to the indicated treatments: vehicle ($n = 5$), gemcitabine (Gem) ($n = 5$), gemcitabine + clodronate ($n = 5$), and gemcitabine + B20 antibody ($n = 4$). ns, not significant.

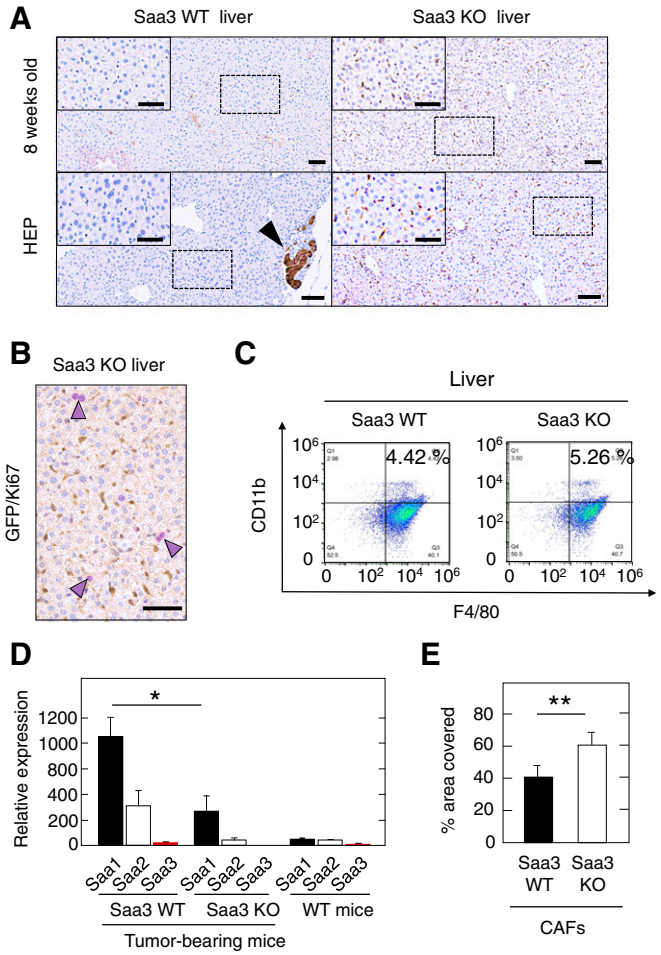

Fig. S4. (*A*) Images of GFP staining in livers of *Saa3*-competent (WT) and *Saa3*-null (KO) KPeCY mice killed at age 8 wk or at the humane end point (HEP). (Scale bars, 100 μm.) *Insets* display high-magnification images of the boxed areas. (Scale bars, 30 μm.) (*B*) Costaining of GFP (brown) and Ki67 (magenta) to mark EYFP$^+$ tumor cells that proliferate (Ki67$^+$) on liver sections of 8-wk-old *Saa3*-null KPeCY mice. (Scale bars, 50 μm.) (*C*) FACS analysis of the macrophage population in livers of 8-wk-old *Saa3*-competent (WT) and *Saa3*-null (KO) KPeCY mice with F4/80 and CD11b antibodies ($n = 4$). (*D*) Expression analysis by qPCR of *Saa* family members in livers of *Saa3*-competent (Saa3 WT) ($n = 3$) and *Saa3*-null (Saa3 KO) ($n = 3$) tumor-bearing KPeCY mice killed at the humane end point and in WT control livers ($n = 2$). Saa1 (solid bars), Saa2 (open bars), and Saa3 (red bars) are indicated. (*E*) Quantitative analysis of migration assays in *Saa3*-competent (WT, solid bar) and *Saa3*-null (KO, open bar) CAFs. The percentages represent the area covered by CAFs 16 h after the generation of the scratch. $^*P < 0.05$; $^{**}P < 0.001$.

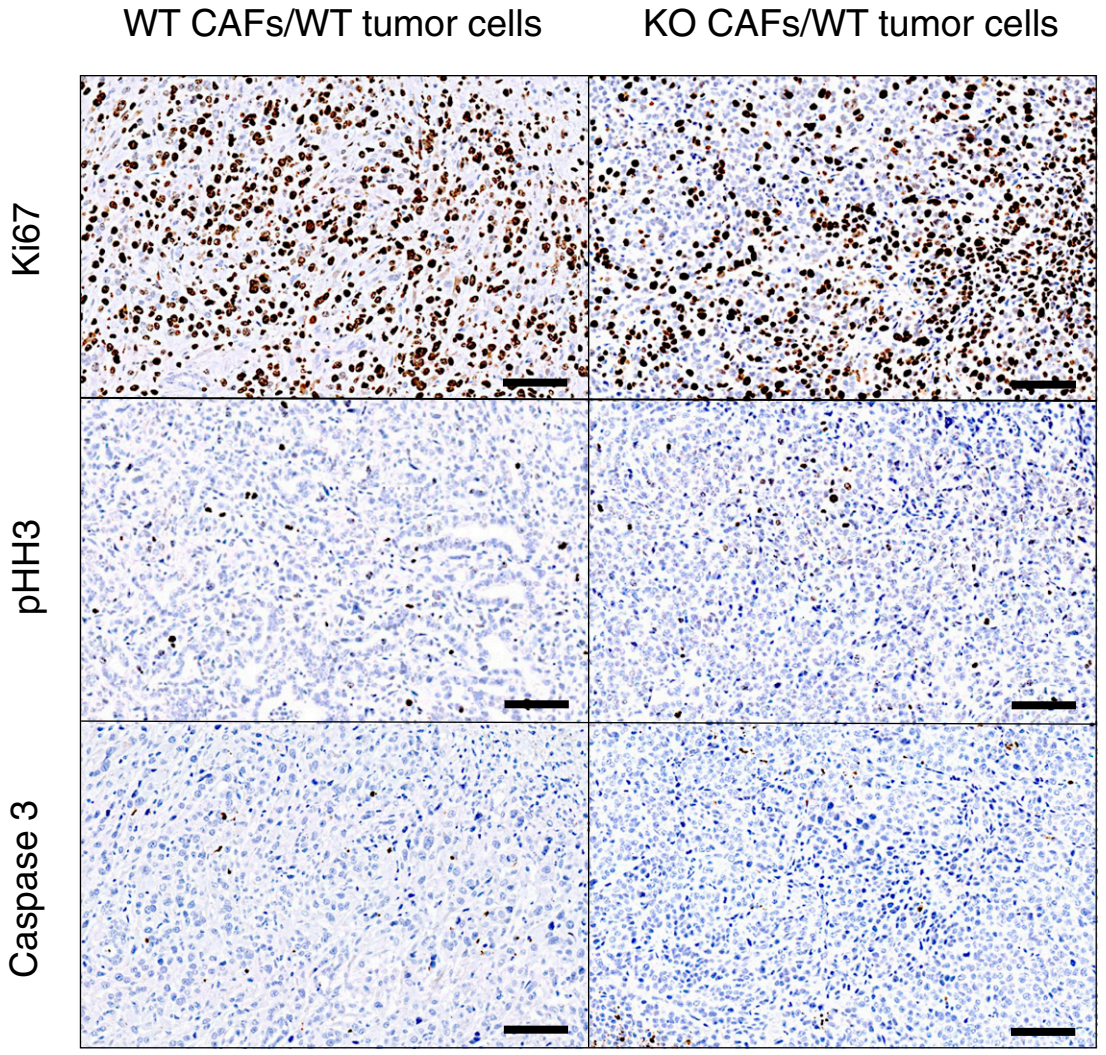

Fig. S5. IHC analysis of sections of orthotopic tumors generated by injecting nude mice with *Saa3*-competent (WT) CAFs along with *Saa3*-competent (WT) tumor cells (*Left*) and *Saa3*-null (KO) CAFs (*Right*) along with *Saa3*-competent (WT) tumor cells. Sections were stained with antibodies against Ki67 (*Top*), pHH3 (*Middle*), and cleaved caspase-3 (*Bottom*). (Scale bars, 50 μm.)

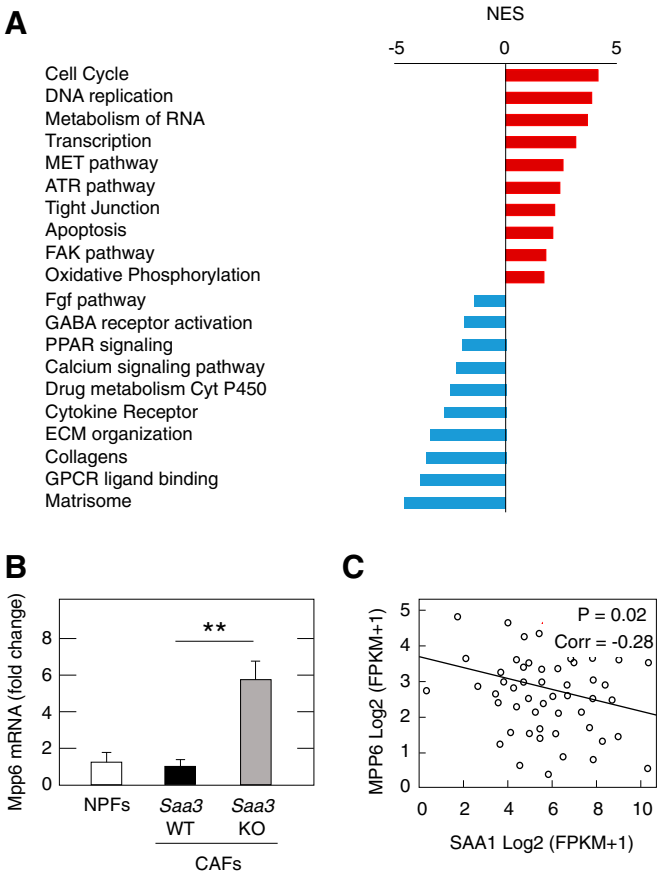

Fig. S6. (*A*) GSEA pathway analysis of *Saa3*-competent vs. *Saa3*-null pancreatic tumor cells including the 10 most significantly up- and down-regulated pathways. The NES ranking was generated by the GSEA. (*B*) qPCR validation of Mpp6 expression levels in NPFs (open bar) and in *Saa3*-competent (WT) (solid bar) and *Saa3*-null (KO) CAFs (gray bar). $^{**}P < 0.001$. (*C*) Correlation of *SAA1* and *MPP6* expression (in FPKM) in Moffitt's dataset. Spearman's correlation (Corr) and *P* value are indicated.